Research Article

Properties of the *N*-terminal domains from Y receptors probed by NMR spectroscopy[‡]

Chao Zou, Sowmini Kumaran, Reto Walser and Oliver Zerbe*

Binding of neurohormones from the NPY family to their receptors, the so-called Y receptors, that belong to the superfamily 1b of G-protein coupled receptors might include transient binding to the *N*-terminal domains of the receptors. Accordingly, we have studied structural features of the *N*-terminal domains from the Y1, Y2, Y4, and Y5 receptor subtypes (*N*-Y1, *N*-Y2, *N*-Y4, *N*-Y5). We developed efficient strategies for their recombinant expression. *N*-Y4 and *N*-Y1 were expressed as insoluble fusions to enforce accumulation into inclusion bodies, whereas *N*-Y2 and *N*-Y5 were expressed as soluble fusion proteins. All *N*-terminal domains are fully flexible in aqueous buffer. In the presence of phospholipid micelles some stretches within the polypeptides adopt helical conformations, but these are too unstable to be characterized in detail. Using chemical shift mapping techniques, interactions of NPY, peptide YY (PYY), and pancreatic polypeptide (PP), the three members of the neurohormone family that are the Y receptors' natural ligands, with *N*-Y1, *N*-Y2, and *N*-Y5 revealed chemical shift changes in all cases, with the largest values being encountered for PP interacting with *N*-Y1 or *N*-Y5 both in the presence and in the absence of phospholipid micelles. The strength of the interactions, however, is generally weak, and the data also point to nonspecific contacts. Previously, in case of the interaction of *N*-Y4 with PP, the contacts were shown to be electrostatic in nature. This work indicates that association of the peptides with the *N*-terminal domains may generally be part of their binding trajectory. Copyright © 2009 European Peptide Society and John Wiley & Sons, Ltd.

Supporting information may be found in the online version of this article

Keywords: GPCR; Y receptors; membrane proteins; structural biology; *N*-terminal domains

Introduction

G-protein coupled receptors (GPCRs) present the pharmacologically most important class of receptors and the most important target for pharmaceutical drugs [1]. Recently, significant progress has been made in structural studies of GPCRs. For example, the structures of bovine rhodopsin [2], the data on the β1 and β2-adrenergic receptors [3,4] and on squid rhodopsin [5] have improved our understanding of this biologically important class of proteins.

Generally, the structure of GPCRs can be described as an extracellular *N*-terminal domain (ranging in size from ten to several thousand residues), which is anchored in the plasmamembrane by 7 transmembrane helices (7TM segment). The latter are interconnected by three intracellular and three extracellular loops. The 7TM segment is followed by a cytoplasmic *C*-terminal domain. Although the extracellular *N*-terminal domain of bovine rhodopsin revealed the non-anticipated presence of a short antiparallel β-sheet, the corresponding segment of the β-adrenergic receptors could not be traced in the electron maps presumably because of its inherent flexibility [3,4].

Previously, we have in detail investigated structural properties of a 41 amino acid fragment corresponding to the *N*-terminal domain of the human Y4 receptor (*N*-Y4) [6]. This receptor belongs to a class of GPCRs targeted by neurohormones of the NPY family [7,8]. The Y receptors are comprised of four subtypes called Y1, Y2, Y4, and Y5 with Y4 showing high affinity and specificity for the pancreatic polypeptide (PP). Although unstructured in solution, a short α-helical stretch comprising residues 5–10

was observed in the presence of phospholipid micelles for *N*-Y4 [6].

In this work, we now report on our recent studies on structural properties of all other *N*-terminal domains from the human Y receptors (for sequences see Figure 1). Synthetic routes for recombinant production of the polypeptides in isotopically labeled form are described and compared with each other. The *N*-terminal domains from all Y receptors are fully unstructured in aqueous solution. On the contrary, in the presence of phospholipid micelles, all *N*-termini except of *N*-Y2 form helical segments with variable degree of stability.

In our previous work, we demonstrated that *N*-Y4 interacts with PP [6]. Surface plasmon resonance (SPR) measurements indicated weak (K_d 50 μM) binding, and subsequent mutagenesis experiments revealed that electrostatic interactions from anionic ligand and cationic *N*-Y4 residues contributed to that interaction. In this work, we also tested binding of the principal members of the NPY family [NPY, PP, and peptide YY (PYY)] to all other Y receptor *N*-terminal domains.

* *Correspondence to: Oliver Zerbe, Institute of Organic Chemistry, University of Zurich, Winterthurerstrasse 190, CH-8057 Zurich, Switzerland.*
  E-mail: oliver.zerbe@oci.uzh.ch

  Institute of Organic Chemistry, University of Zurich, Winterthurerstrasse 190, CH 8057 Zurich, Switzerland

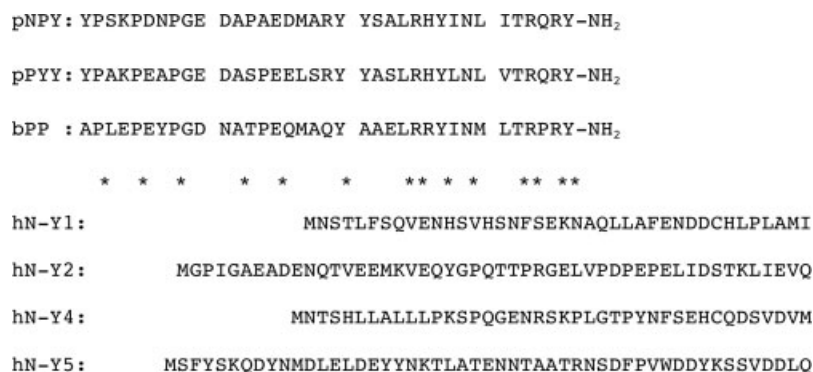‡ *11th Naples Workshop on Bioactive Peptides.*

```
pNPY: YPSKPDNPGE DAPAEDMARY YSALRHYINL ITRQRY-NH₂

pPYY: YPAKPEAPGE DASPEELSRY YASLRHYLNL VTRQRY-NH₂

bPP : APLEPEYPGD NATPEQMAQY AAELRRYINM LTRPRY-NH₂

       *  *   *    *  *    *    ** *  *   ** **

hN-Y1:                  MNSTLFSQVENHSVHSNFSEKNAQLLAFENDDCHLPLAMI

hN-Y2:         MGPIGAEADENQTVEEMKVEQYGPQTTPRGELVPDPEPELIDSTKLIEVQ

hN-Y4:            MNTSHLLALLLPKSPQGENRSKPLGTPYNFSEHCQDSVDVM

hN-Y5:      MSFYSKQDYNMDLELDEYYNKTLATENNTAATRNSDFPVWDDYKSSVDDLQ
```

Figure 1. Sequence alignment of the principal members of the NPY family and of the *N*-terminal domains from the various Y receptor subtypes.

Materials and Methods

$^{15}NH_4Cl$ was from Spectra Isotopes (Columbia, USA), d_{13}-MES, d_{38}-dodecylphosphocholine (d_{38}-DPC) (99%-d), and D_2O was from Cambridge Isotope Laboratories (Andover, Massachusetts, USA). 5-doxylstearic acid was from Aldrich (Buchs, Switzerland). Oligonucleotide primers were synthesized by Microsynth GmbH (Balgach, Switzerland).

Expression and Purification of *N*-terminal Domains from the Human Y Receptors

Depending on their stability against proteolysis, the *N*-terminal domains were either expressed as fusions to ubiquitin (*N*-Y2 and *N*-Y5) or to ketosteroidisomerase (KSI) (*N*-Y1 and *N*-Y4).

In case of *N*-Y2 and *N*-Y5, the amino acid sequence was reverse translated into a DNA sequence taking into account the preferred *Escherichia coli* codon usage including a terminal stop codon and a *Sal*I restriction site. The resulting fragments were purified by electrophoresis and gel extraction and digested with *Sal*I, resulting in fragments that were blunt-ended on one side and contain a *Sal*I-cohesive end on the other end. These fragments were ligated into the pUBK19 vector (gift from T. Kohno, Mitsubishi Kasei Institute of Life Science, Tokyo, Japan), which had been digested with *Nsi*I and *Sal*I and purified before. The resulting plasmids were sequenced and transformed into C41 cells [9]. For production of ^{15}N-labeled peptides, M9 minimal medium containing ^{15}N-ammonium chloride as the sole nitrogen source was used, otherwise expression was done on LB medium. In each case, 1 l of medium containing 50 µg/ml kanamycin was inoculated with 10 ml of an overnight LB culture. Cultures were induced at OD_{600} around 0.5 with 0.4 mM IPTG. LB and minimal medium cultures were grown under induction for 4 and 11 h, respectively. Cells were harvested by centrifugation at 4 °C and stored at −20 °C. The cell pellets were thawed on ice for 1 h and resuspended in 25 ml of denaturing basic buffer (50 mM Tris, pH 8; 6 M GdnHCl; 100 mM NaCl; 1 mM β-mercaptoethanol). The cells were lysed by sonication on ice.

The ubiquitin fusion proteins were purified by Ni-NTA chromatography. Refolding was achieved by applying a linear gradient to exchange the denaturing basic buffer to native binding buffer (50 mM Tris, pH 8; 100 mM NaCl; 1 mM β-mercaptoethanol, 20 mM imidazole), and the protein was eluted with binding buffer containing 200 mM imidazole. The eluates were diluted 10-fold with basic buffer (50 mM Tris, pH 8; 100 mM NaCl; 1 mM β-mercaptoethanol) and a 1 mg/ml yeast ubiquitin hydrolase (YUH) solution (for expression and purification of YUH see Supporting Information) was

added in a 20-fold dilution. The cleavage reactions were allowed to proceed for 3 h at 37 °C.

In case of *N*-Y1 and *N*-Y4, the DNA sequences were subcloned from wt cDNA of the corresponding Y receptor (University of Missouri-Rolla (UMR) cDNA Resource Center) by PCR. During PCR, a GSGSGS linker followed by a tobacco etch virus (TEV) cleavage sequence was introduced at the *N*-terminus of the target sequence. After digestion with *Xho*I and *Esp*I, the fragments were ligated with T4 DNA ligase into the pET31b vector, which had been digested with *Xho*I and *Esp*I. The correctness of the constructs was verified by DNA sequencing (Synergene Biotech, Switzerland). The resulting plasmids were transformed into BL21(DE3) for expression. For production of ^{15}N-labeled peptides, M9 minimal medium containing ^{15}N-ammonium chloride as the sole nitrogen source was used, otherwise expression was done in LB medium. In each case, 1 l of medium containing 50 µg/ml kanamycin was inoculated with 10 ml of an overnight LB culture. Cultures were induced at OD_{600} of 0.7 with 1 mM IPTG, harvested after 5 h by centrifugation on a Sorval GSA rotor at 4 °C and the pellets were stored at −20 °C.

The fusion proteins were purified from inclusion bodies by Ni–NTA chromatography in presence of 6 M GdnHCl. After removal of GdnHCl by dialysis, the precipitated fusion protein was solubilized in 50 mM Tris, pH 8.0, in the presence of 2% *N*-lauryl sarcosine upon sonication to a final concentration of 2 mg/ml. The resulting solution was dialyzed against a 20-fold excess of 50 mM Tris, pH 8.0, for 4–6 times. The solution was diluted 10 times with 50 mM Tris, pH 8.0, and EDTA and DTT were added to a final concentration of 0.5 mM and 1 mM, respectively. TEV protease (for expression and purification of TEV protease see Supporting Information) was added to a final concentration of 100 mM and the cleavage mixture was incubated at 4 °C over night.

All target peptides were finally purified by C18-RP-HPLC (Vydac, USA) by using a water/acetonitrile/0.1% TFA gradient. Yields ranged from 3 to 20 mg peptide from 1 l of culture. The mass of all peptides was confirmed by MALDI–TOF MS or ESI–MS: *N*-Y1: 4532.9 Da (theoretical value: 4533.0 Da); ^{15}N-*N*-Y1: 4587.0 Da (theoretical value: 4587.0 Da); *N*-Y2: 5509.3 Da (theoretical value: 5510.0 Da); ^{15}N-*N*-Y2: 5568.0 Da (theoretical value: 5570.0 Da); *N*-Y4: 4554.0 Da (theoretical value: 4556.1 Da); ^{15}N-*N*-Y4: 4614.0 Da (theoretical value: 4611.1 Da); *N*-Y5: 6053.7 (theoretical value: 6053.4); ^{15}N-*N*-Y5: 6119.5 Da (theoretical value: 6118.4 Da).

NMR and CD Spectroscopy

For studies of structure or backbone dynamics, 1 mM solutions of the peptides at pH 5.6, 20 mM d_{13}-MES, and 300 mM d_{38}-DPC

were used. All spectra were recorded on an AV-700 Bruker NMR spectrometer at 310 K. Chemical shifts were calibrated to the water line at 4.63 ppm and nitrogen shifts were referenced indirectly to liquid NH_3 [10]. The spectra were processed using the Bruker Topspin2.0 software and transferred into the XEASY [11] or CARA [12] programs for further analysis.

For chemical shift assignments, 3D ^{15}N-resolved TOCSY and NOESY [13] were used. In case of *N*-Y5, we decided to use ^{13}C,^{15}N labeling in combination with experiments that directly correlate sequential amide moieties [14]. Upper-distance limits for structure calculations of *N*-Y1 were derived from a 70-ms NOESY spectrum [15]. Structures were calculated in the program CYANA using its standard simulated annealing protocol [16].

A proton-detected version of the steady-state ^{15}N{^{1}H} heteronuclear Overhauser effect sequence was used for measurement of the heteronuclear NOE [17]. Therein, the buildup of the NOE was achieved through a pulse train of 120° proton pulses separated by 5 ms over a period of 3 s.

For measurements of interactions by chemical shift mapping methodology, 0.1 mM solutions of the ^{15}N-labeled neurohormones were mixed with the corresponding peptides from the *N*-terminal domains at pH 5.6, 20 mM d_{13}-MES, 300 mM d_{38}-DPC, and the deviations of peak positions were extracted from the [^{15}N,^{1}H]-HSQC spectra and computed according to $\Delta\delta = \text{SQRT}(\Delta(^1\text{H})^2 + 0.2 \times \Delta(^{15}\text{N})^2)$. Particular care was taken to ensure that no shifts in pH occurred when adding the *N*-Y peptides. In case of addition of various equivalents of pNPY to ^{15}N-labeled *N*-Y2 in the presence of DPC micelles, the sample was prepared in 20 mM d_{13}-MES, 300 mM d_{38}-DPC at pH 5.6 and pNPY was added as a solid.

For CD analysis, a certain amount of peptides was dissolved in 300 mM DPC buffered with 20 mM MES (pH 5.6), such that the far UV absorption was around 1. CD spectra were recorded at 37 °C on a Jasco model J-810 using a quartz cuvette with path length of 1 mm to minimize absorption by the detergent. All spectra were averaged from three consecutive measurements in the range between 190 and 250 nm with a slit width of 1 nm and a scanning rate of 5 nm/min. The blank sample was recorded under identical conditions and subtracted from the sample spectra. The final CD intensity is expressed as mean residue ellipticity (degree cm^2/dmol).

Results

Expression of *N*-terminal Domains in Isotopically Labeled Form

Isotope labeling of the investigated peptides was required for the study of backbone dynamics using ^{15}N relaxation and for chemical shift mapping experiments for the study of macromolecular interactions. Such labeling precludes the usage of peptides produced from solid phase synthesis and necessitates recombinant production. For reasons of simplicity, we generally prefer *E. coli* as the expression host [18]. To avoid rapid degradation in *E. coli*, the peptides need to be linked to a (more) stable fusion partner [19] (Figure 2). Specific cleavage from the fusion partner can be accomplished for systems for which a specific hydrolase (e.g. a ubiquitin hydrolase) is available or by introducing a unique cleavage site, either a protease-sensitive site or a site prone to cleavage by chemicals such as CNBr [20] or hydroxylamine [21]. CNBr cleavage in our case was incompatible with the presence of Met residues, and poor efficiency was observed with hydroxylamine, and therefore enzymatic cleavage had to be used. However, the latter methods require that the fusion protein should be solubilized under conditions that are compatible with enzymatic activity.

Because the four Y receptor *N*-terminal fragments studied herein are all reasonably water-soluble and contain Met residues, we initially decided to express them in ^{15}N-labeled form as *C*-terminal fusions to *N*-terminally decahistidine-tagged yeast ubiquitin [22]. After purification of the fusion construct by Ni-affinity chromatography, the desired peptide was liberated through treatment with YUH. This system allowed the recovery
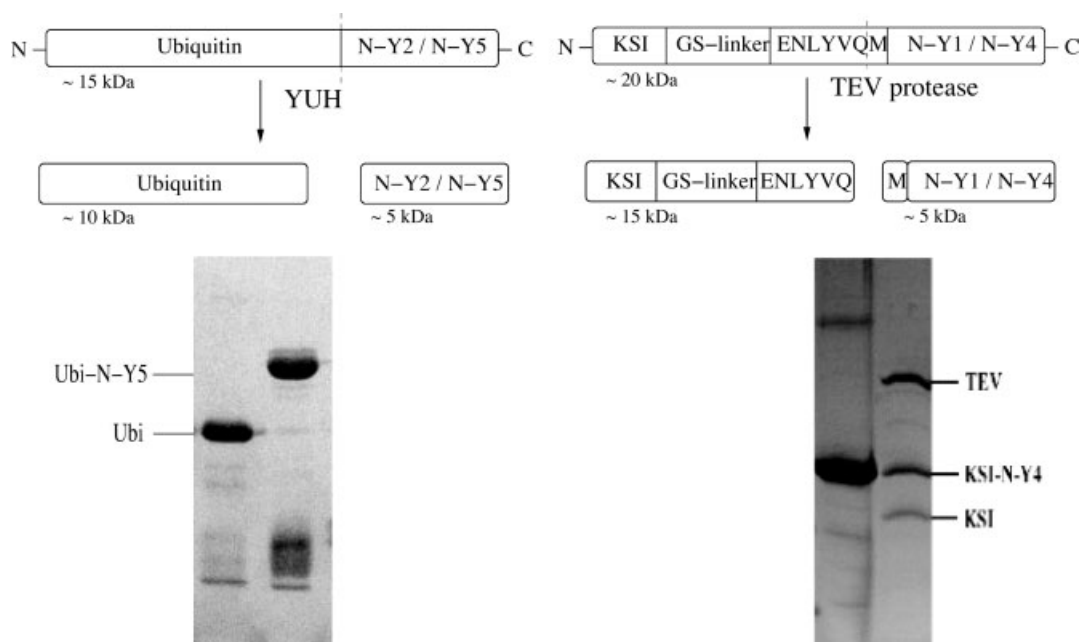

Figure 2. Scheme showing the two strategies used to produce peptides corresponding to the *N*-terminal domains of the Y receptors and examples from *N*-Y5 and *N*-Y4 for the corresponding scheme, respectively.
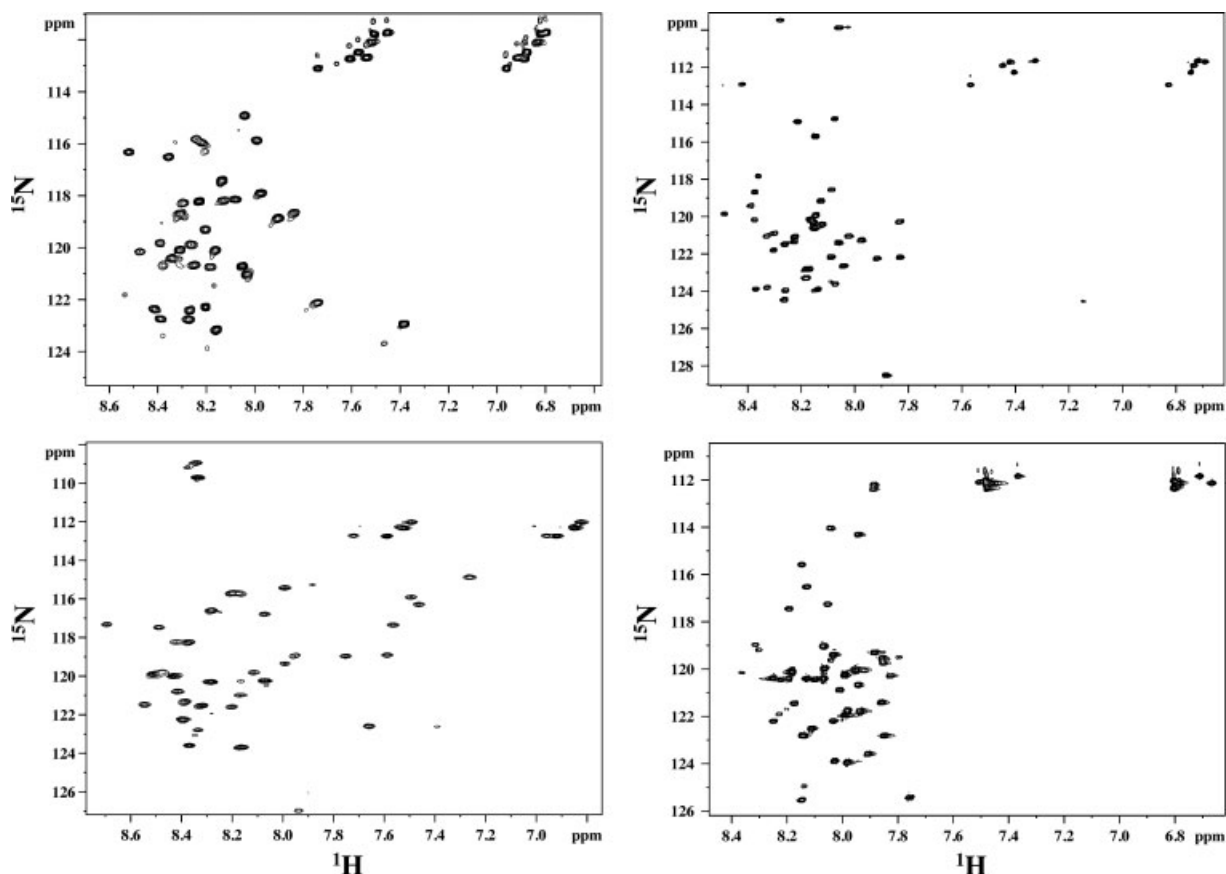
Figure 3. [^{15}N,^{1}H]-HSQC spectra of all Y receptor *N*-terminal domains, recorded at 310 K in the presence of DPC micelles. Top left: *N*-Y1, top right: *N*-Y2, bottom left: *N*-Y4, bottom right: *N*-Y5.

of about 6 mg of ^{15}N-labeled *N*-Y2 and *N*-Y5 from 1 l of culture. Unfortunately, attempts to express *N*-Y1 and *N*-Y4 using this method resulted in unspecific *C*-terminal degradation. To circumvent intracellular proteolysis, *N*-Y1 and *N*-Y4 were expressed as a fusion to the highly water-insoluble protein KSI, which resulted in accumulation of the fusion protein in inclusion bodies. A TEV protease cleavage site was introduced between KSI and target peptide [23,24]. The sequence recognized by the TEV protease is ENLYFQ with Q as the P1′ residue. To achieve the natural peptide sequence after cleavage, the P1′ residue was replaced with the first residue from the target sequence (here it is Met) [23], and an additional GSGSGS linker was inserted between KSI and the TEV cleavage site to prevent steric hindrance during cleavage.

A problem of the chosen strategy was that the water-insoluble fusion protein had to be solubilized in detergent that is compatible with activity of the TEV protease [25]. After extensive detergent screening, we observed that the ionic detergent sarcosyl solubilizes the fusion protein while preserving TEV protease activity to a satisfactory extent. Cleavage efficiency for this system is around 40% allowing recovery of about 2 mg of ^{15}N-labeled *N*-Y1 and *N*-Y4 from 1 l of bacterial culture.

Assignment of Chemical Shifts

Sequence-specific resonance assignments were done using the strategy developed by Wüthrich *et al*. [26]. Owing to extensive resonance overlap of the poorly folded peptides ^{15}N-resolved 3D TOCSY or NOESY data had to be utilized for this task.

Representative [^{15}N,^{1}H]-HSQC spectra of all four peptides are depicted in Figure 3. In case of *N*-Y5 a ^{13}C,^{15}N-labeled sample, allowing the acquisition of triple resonance spectra, was required. For *N*-Y1, a set of experiments were first recorded in aqueous buffer. After completed analysis in water, the assignments were adjusted to the spectra recorded in the presence of DPC micelles with the help of NOESY spectra. Chemical shifts have been deposited in the BMRB database under accession codes 80.8933262 (*N*-Y1), 80.6873033 (*N*-Y2), and 80.74817093 (*N*-Y5).

Screening Structural Properties Using ^{15}N Relaxation and CD Spectroscopy

CD spectroscopy is a convenient tool to estimate the type and content of secondary structure in peptides and proteins. The CD spectra of all *N*-terminal domains in the presence of DPC micelles are depicted in Figure 4. The spectrum of *N*-Y2 displays its minimum around 197 nm, the typical absorption band of unstructured peptides. For all other peptides, the minimum is red-shifted and indicates population of helical substructures. The intensities of the absorptions, however, also clearly show that the helical content is very low in all cases, and the typical double minimum at 208 and 222 nm is not visible. For *N*-Y4, for which we previously observed an α-helix involving residues 5–10, the absorption is stronger than for the other peptides.

The dispersion of the NMR signals in the region of the amide protons is traditionally used to estimate to which extent a peptide or protein is folded [27]. In case of the *N*-terminal domains from the
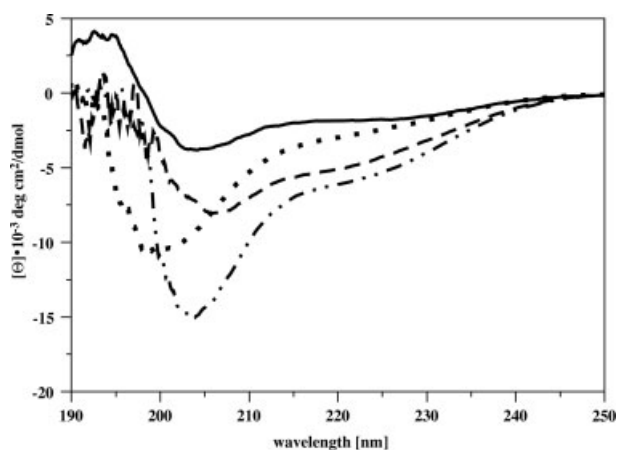
Figure 4. CD spectra of peptides from all *N*-terminal domains, recorded at 37 °C in 300 mM DPC, 20 mM MES pH 5.6 solution. Data are shown for *N*-Y1 (solid line), *N*-Y2 (dotted line), *N*-Y4 (dash-dotted line), and *N*-Y5 (dashed line). Data are converted to mean residue ellipticities.

Y receptors, signal dispersion of all peptides was small, indicating that they were largely unfolded. To better assess whether these peptides still contained folded segments, we recorded the ^{15}N{^{1}H}-NOEs (H-NOEs). These values range from 0.6 to 0.8 for well-folded elements of secondary structures, and progressively decrease for more flexible amide moieties resulting in negative values for fully flexible segments [28]. The H-NOE data for all *N*-terminal peptides reveal that all peptides are essentially unstructured in aqueous buffer (data not shown).

Because in the naturally occurring GPCR, the *N*-termini are attached to a membrane protein, the backbone dynamics were additionally probed in the presence of a commonly used membrane-mimicking detergent, DPC [29] (Figure 5). Again, the peptides are not rigidly structured. In the case of *N*-Y4, we could previously show that a rather stable hydrophobic α-helix is formed between residues 5 and 10, present both in zwitter ionic (DPC) as well as in anionic (SDS) micelles [6], reflected by H-NOEs exceeding values of 0.6. On the contrary, the *N*-termini from all other Y receptors are less well ordered. The *N*-Y2 is fully flexible most likely due to the complete lack of interactions with phospholipid surfaces. The absence of such contacts is supported by the fact that essentially no chemical shift changes occur between *N*-Y2 in aqueous buffer and in DPC micelles. On the contrary, both *N*-Y1 and *N*-Y5 reveal short stretches of the polypeptide chain that become rigidified in the presence of the micelles.

The Structures of the *N*-terminal Domains in the Presence of Phospholipid Micelles

The H-NOE data of *N*-Y4 revealed the presence of a hydrophobic helix in the segment comprising residues 5–10. In addition, a nascent helix was observed in the region including residues 26–35. Inspection of the H-NOE data depicted in Figure 5 clearly indicates that *N*-Y2 is devoid of any structured segments. Moreover, the H-NOE of *N*-Y5 is generally below 0.6 and mostly values are even smaller than 0.4. In our experience, secondary structure cannot reliably be determined in these cases. We speculate that the molecule, similarly to *N*-Y4, is segregated into a *N*-terminal helical region, and a much more destabilized shorter *C*-terminal helical region separated by a longer non-ordered segment, but the peptide is not ordered sufficiently well to allow for structural characterization by NMR in detail.

In case of *N*-Y1, however, elevated values of the H-NOE are observed indicating that this polypeptide may be amenable to more detailed structural studies. Accordingly, we have assigned all proton and nitrogen resonances of *N*-Y1. During assignment, a larger number of contacts involving sequential amide protons were observed, indicating that the ϕ, ψ space of helical backbone conformations was significantly populated. Such stretches were, for example, observed for residues 4–9 and residues 24–32. An expansion of the spectral region of the [^{1}H,^{1}H]-NOESY that displays the sequential amide proton NOEs in the segment from 24 to 32 is shown in Figure S5 in the Supporting Information. However, except for two α,N (i,i + 3) NOEs observed in the segment 4–9, no medium-range contacts were found. The relative strength of intraresidual and sequential αH,NH contacts changes between extended and helical conformations [30], with the intraresidual distance in helices stronger than the sequential one, whereas in extended or unfolded segments the sequential distance is much shorter. A comparison of peak intensities revealed that the sequential αH,NH NOEs were generally stronger, and in the light of sequential NH,NH contacts, indicate conformational averaging between helical and extended conformations to some extent. Considering this observation, it was not really surprising that persistent violations remained in the structure calculations, and helical conformations were only seen involving residues 4–9, a region, in which the H-NOE is larger than 0.6. The ^{3}J(HN,Hα) couplings were larger than 6.5 Hz throughout the sequence (data not shown), reflecting the remaining conformational instability of *N*-Y1. To our surprise, we have not been able to detect any medium-range contacts in the segment 15–28, which according to the dynamics data should also be better ordered. We suspect this region to be transiently helical considering the occurrence of sequential amide proton contacts throughout this segment.

To summarize, the spectroscopic data indicate that *N*-Y4 and *N*-Y5 are similar in that both contain two helical regions separated by a flexible central segment, with only the *N*-terminal helix in *N*-Y4 being well ordered. *N*-Y1 is largely helical between residues 4 and 28, but the remaining conformational flexibility precludes its detailed structural analysis. *N*-Y2 is fully flexible and devoid of any detectable residual structure.

Interaction Studies with Neuropeptides from the NPY Family

We have recently proposed that the peptides of the NPY family may transiently bind to the *N*-terminal domains of Y receptors in order to become transferred from the membrane-bound state into the genuine binding pocket of the receptor [6,31]. Although in that work SPR was used to establish the strength of the bPP–NY4 (b: bovine) interaction, preliminary experiments using bPP or pPYY (p: porcine) and *N*-terminal domains from the other receptors have indicated that the interaction between the peptides and the other *N*-terminal domains are too weak to be detected by SPR. We have also tried to apply isothermal titration calorimetry but reproducibility of the data recorded in presence of micelles was very unsatisfying, most likely related to the fact that this technique in detergent becomes very challenging when the dissociation constant is more than 10 μM. Therefore, we utilized chemical shift mapping experiments both in presence and absence of DPC micelles in order to derive preliminary data on binding of the peptides from the NPY family to *N*-Y1, *N*-Y2, and *N*-Y5 (Figure S11, Supporting Information). To briefly summarize these experiments, we note that in case of pPYY changes are similar (but small) for all *N*-terminal domains, whereas in case of bPP,
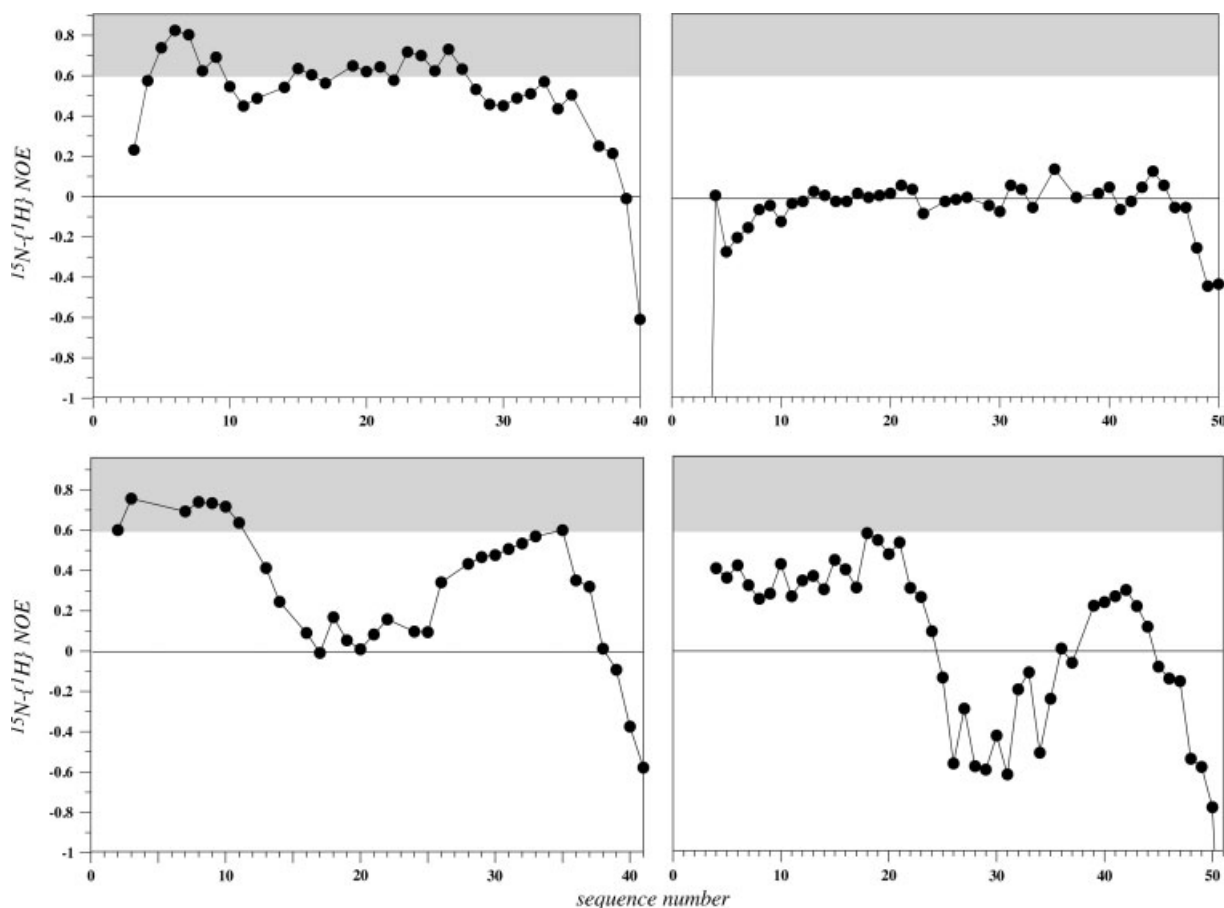
Figure 5. Values of the ^{15}N-{^{1}H}-NOE, recorded at 700 MHz proton frequency along the sequence for Y1 (top left), Y2 (top right), Y4 (bottom left), and Y5 (bottom right). The area containing values larger than 0.6, indicating rather well-folded segments, has been shaded in gray.
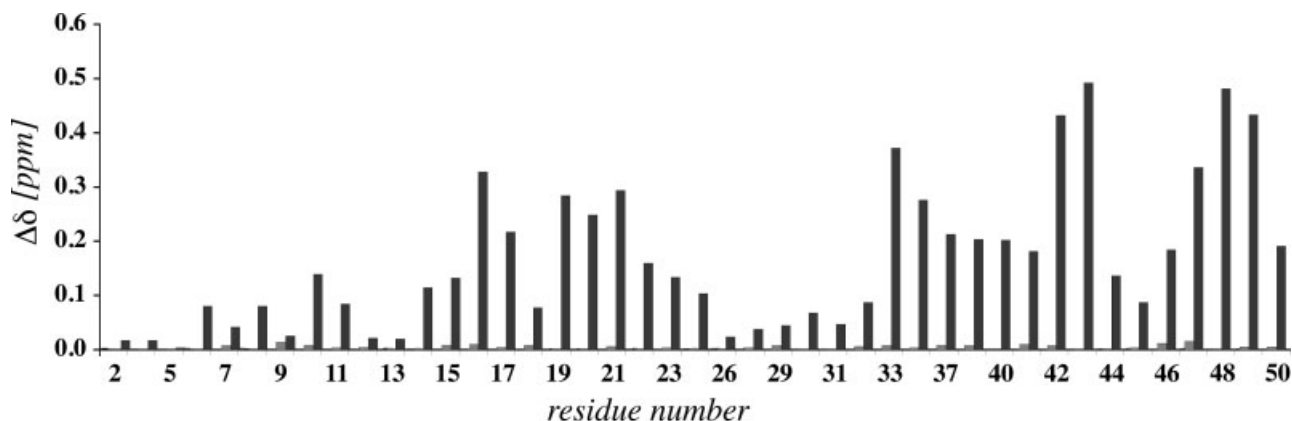

Figure 6. Chemical shift deviation of *N*-Y2 after addition of 1 and 10 equivalents of pNPY (from left to right). For additional data points at 0.5, 2, and 4 equivalents, see Figure S11 in the Supporting Information.

N-Y1 or *N*-Y5 behave differently compared with *N*-Y4 [32–34]. To investigate whether pNPY really associates with *N*-Y2, we have performed a titration experiment, in which up to 10 equivalents of pNPY were added to ^{15}N-labeled *N*-Y2 (Figure 6). The data clearly show concentration-dependent changes of positions of resonances from *N*-Y2. Resonances in the segments comprising *N*-Y2 residues 16–21 and 33–50 are mostly affected. We noticed that acidic residues Glu and Asp are particularly numerous among the residues showing large chemical shift changes when pNPY

is added in large excess. This might point to rather nonspecific electrostatic contributions to the weak interaction between *N*-Y2 and pNPY, a fact that has been also observed for the interaction of *N*-Y4 with bPP. To summarize the interaction studies, we can say that significant and reliable effects were only detected in the presence of DPC micelles, and that the interaction of bPP with *N*-Y4 is much stronger than for the other *N*-termini, and for all other possible interactions of NPY or PYY with the *N*-terminal peptides.

Discussion

We have postulated that binding of ligands to Y receptors is preceded by association of the ligands with the plasma membrane. Thereby, the apparent concentration of the ligand in vicinity of the receptor is increased and the search for the receptor reduced from three to two dimensions [35–37]. We now studied whether parts of the receptor that protrude into the extracellular compartment may help in transferring ligands, which have accumulated in vicinity of the membrane, into the binding pocket. Such portions of receptors that point into the extracellular space are the *N*-terminal domains. Herein, we have developed strategies to produce these polypeptides recombinantly in isotopically enriched form for use in high-resolution NMR studies.

The work has demonstrated that these peptides can all be expressed as soluble fusions to ubiquitin. However, *N*-Y4 and *N*-Y1 are degraded in the intracellular milieu, and hence much better yields were obtained using insoluble fusions. Cleavage of the target sequence from the insoluble fusion partner could be achieved by solubilizing the fusion protein in the mild detergent sarcosyl, which proved to be compatible with enzymatic activity of the TEV protease used to cleave the peptide from the fusion protein.

Studies on the structure and dynamics of the peptides using NMR revealed that they are all completely disordered in aqueous buffer. In the presence of phospholipid micelles, segments of most receptor *N*-termini became conformationally stabilized, with the exception of *N*-Y2, which remained unstructured. Otherwise, more (*N*-Y4) or less stable (*N*-Y1 or *N*-Y5) helical segments occurred within the sequences. For all *N*-terminal peptides, chemical shift changes occurred between spectra recorded in presence and absence of DPC micelles, except for *N*-Y2. This implies that all other peptides associate with the micelle to some extent. Previously, we have made extensive use of the thermodynamic data of Wimley and White for partitioning of single amino acids into the water-membrane interface or the membrane interior [38] to rationalize how peptides interact with phospholipid micelles. A common observation was that the occurrence of the aromatic residues Trp and Tyr helps in anchoring peptides in the interface [39]. The partitioning values of the four sequences of the *N*-terminal domains from the Y receptor subtypes are shown in Figure S6 in the Supporting Information. In *N*-Y4, a stretch comprising residues 5–11 is predicted to show partitioning into the micelle interior. This corresponds exactly to the region that becomes helically structured in the presence of micelles. In case of *N*-Y2, many negatively charged residues occur throughout the sequence, whereas they are clustered in the central (unstructured) segment in *N*-Y4. Even more importantly, many Pro residues are present in *N*-Y2 that might prevent formation of secondary structure. The sequence of *N*-Y5 in comparison with *N*-Y2 is much more amphiphilic in nature, and therefore more likely to favorably interact with the micelles. Again, the regions that become better structured in the presence of DPC micelles correspond to stretches rich in hydrophobic/aromatic residues and hence are predicted to partition into the micelles. The fact that the *N*-termini of the Y receptors are largely unstructured is compatible with present structural knowledge derived from crystal structures of class-A GPCRs [2,4,5,40,41]. Therein, the *N*-termini are rather flexible. However, a short two-stranded antiparallel β-sheet complementing the β-sheet formed by residues of the long E2 loop is encountered in bovine rhodopsin [2], whereas a very short helix is present in squid rhodopsin [5]. In both β-adrenergic receptors, the *N*-terminal portions are not defined in the crystal structures [4,41].

Our interaction studies using chemical shift mapping indicated that bPP strongly interacts with all *N*-terminal domains, but differences in the sensitivity of certain positions are observed. On the contrary, for pPYY or pNPY the changes are smaller. In our BiaCore measurements, we could detect strongest binding (K_d ~50 µM) for the bPP–NY4 interaction, and chemical shift mapping also revealed the largest changes for bPP upon addition of *N*-Y4. The fact that the interaction between bPP and N-Y4 is much stronger (K_d 50 µM) than for any other combination of neurohormone and *N*-terminal domain could indicate that this contact additionally contributes to binding in the pocket, and may help to explain why binding of PP to the Y4 receptor is much tighter than binding of PP to the other subtypes, or stronger than binding of NPY or PYY to all Y receptors. Otherwise, we generally see a rather weak nonspecific electrostatic interaction. Whether these interactions are strong enough to really help promoting the membrane-bound peptides into the receptor-binding pocket is unclear based on these data. It is, however, unlikely that they significantly contribute to binding in the genuine binding pocket. Very recently, Beck-Sickinger *et al.* investigated mutants of the Y receptor, in which the *N*-termini were truncated [42]. Their data indicate little loss of binding affinity and signal transduction in the truncated mutants except for the Y2 receptor. Whether these observations indicate that diffusion of the ligand from the membrane-bound state into the receptor-binding pocket may proceed via different, alternative pathways, will need to be subject to further studies.

To summarize, this work has described synthetic methods to produce all *N*-terminal domains in isotopically labeled form in quantities sufficient for the analysis by various biophysical methods. Structural studies revealed them to be fairly flexible. However, although *N*-Y2 is fully unfolded, residual helical structures were detected in *N*-Y1 and *N*-Y5. For the case of *N*-Y4, we could previously detect a short rather rigid α-helical stretch in the presence of DPC micelles. In contrast to *N*-Y4, the nascent helical regions of *N*-Y1 and *N*-Y5 contain too much residual motion, so that structure calculations did not fully converge towards α-helical structures. All peptides interact with the *N*-terminal domains of *N*-Y1, *N*-Y2, and *N*-Y5, but the interactions are weaker than those previously described for bPP binding to *N*-Y4.

Supporting information

Supporting information may be found in the online version of this article.

References

1. Ma P, Zemmel R. Value of novelty? *Nat. Rev. Drug Discov.* 2002; **1**: 571–572.
2. Palczewski K, Kumasaka T, Hori T, Behnke CA, Motoshima H, Fox BA, Le Trong I, Teller DC, Okada T, Stenkamp RE, Yamamoto M, Miyano M. Crystal structure of rhodopsin: A G protein-coupled receptor. *Science* 2000; **289**: 739–745.
3. Cherezov V, Rosenbaum DM, Hanson MA, Rasmussen SG, Thian FS, Kobilka TS, Choi HJ, Kuhn P, Weis WI, Kobilka BK, Stevens RC. High-resolution crystal structure of an engineered human beta2-

adrenergic G protein-coupled receptor. *Science* 2007; **318**: 1258–1265.

4. Rasmussen SGF, Choi HJ, Rosenbaum DM, Kobilka TS, Thian FS, Edwards PC, Burghammer M, Ratnala VRP, Sanishvili R, Fischetti RF, Schertler GFX, Weis WI, Kobilka BK. Crystal structure of the human beta(2) adrenergic G-protein-coupled receptor. *Nature* 2007; **450**: 383–3U4.

5. Murakami M, Kouyama T. Crystal structure of squid rhodopsin. *Nature* 2008; **453**: 363–U33.

6. Zou C, Kumaran S, Markovic S, Walser R, Zerbe O. Studies of the structure of the N-terminal domain from the Y4 receptor, a G-protein coupled receptor, and its interaction with hormones from the NPY family. *ChemBioChem* 2008; **9**: 2276–2284.

7. Larhammar D. Structural diversity of receptors for neuropeptide Y, peptide YY and pancreatic polypeptide. *Regul. Pept.* 1996; **65**: 165–174.

8. Larhammar D, Salaneck E. Molecular evolution of NPY receptor subtypes. *Neuropeptides* 2004; **38**: 141–151.

9. Miroux B, Walker JE. Over-production of proteins in *Escherichia coli*: mutant hosts that allow synthesis of some membrane proteins and globular proteins at high levels. *J. Mol. Biol.* 1996; **260**: 289–298.

10. Live DH, Davis DG, Agosta WC, Cowburn D. Observation of 1000-fold Enhancement of ^{15}N NMR via Proton-Detected Multiple-Quantum Coherences: Studies of Large Peptides. *J. Am. Chem. Soc.* 1984; **106**: 6104–6105.

11. Bartels C, Xia TH, Billeter M, Güntert P, Wüthrich K. The program XEASY for computer-supported spectral analysis of biological macromolecules. *J. Biomol. NMR* 1995; **6**: 1–10.

12. Keller R. *The Computer Aided Resonance Assignment*. CANTINA Verlag: Goldau, 2004.

13. Marion D, Driscoll PC, Kay LE, Wingfield PT, Bax A, Gronenborn AM, Clore GM. Overcoming the overlap problem in the assignment of ^{1}H NMR spectra of larger proteins by use of three-dimensional heteronuclear ^{1}H-^{15}N Hartmann-Hahn multiple-quantum coherence and nuclear overhauser-multiple quantum coherence spectroscopy: Application to Interleukin 1β. *Biochemistry* 1989; **28**: 6150–6156.

14. Weisemann R, Rüterjans H, Bermel W. 3D triple-resonance NMR techniques for the sequential assignment of NH and ^{15}N resonances in ^{15}N- and ^{13}C-labelled proteins. *J. Biomol. NMR* 1993; **3**: 113–120.

15. Kumar A, Ernst RR, Wüthrich K. A two-dimensional nuclear Overhauser enhancement (2D NOE) experiment for the elucidation of complete proton-proton cross-relaxation networks in biological macromolecules. *Biochem. Biophys. Res. Commun.* 1980; **95**: 1–6.

16. Güntert P. Automated NMR structure calculation with CYANA. *Methods Mol. Biol.* 2004; **278**: 353–378.

17. Noggle JH, Schirmer RE. *The Nuclear Overhauser Effect – Chemical Applications*. Academic Press: New York, 1971.

18. Sahdev S, Khattar SK, Saini KS. Production of active eukaryotic proteins through bacterial expression systems: a review of the existing biotechnology strategies. *Mol. Cell. Biochem.* 2008; **307**: 249–264.

19. LaVallie ER, McCoy JM, Smith DB, Riggs P. Enzymatic and chemical cleavage of fusion proteins. *Curr. Protoc. Mol. Biol.* 2001; **16**: 4.9–4.17.

20. Kulioulos A, Walsh CT. Production, purification and cleavage of tandem repeats of recombinant peptides. *J. Am. Chem. Soc.* 1994; **116**: 4599–4607.

21. Bornstein P, Balian G. Cleavage at Asn-Gly bonds with hydroxlyamine. *Methods Enzymol.* 1977; **47**: 132–145.

22. Kohno T, Kusunoki H, Sato K, Wakamatsu K. A new general method for the biosynthesis of stable isotope-enriched peptides using a decahistidine-tagged ubiquitin fusion system: an application to the production of mastoparan-X uniformly enriched with ^{15}N and ^{15}N/^{13}C. *J. Biomol. NMR* 1998; **12**: 109–121.

23. Kapust RB, Tozser J, Copeland TD, Waugh DS. The P1′ specificity of tobacco etch virus protease. *Biochem. Biophys. Res. Commun.* 2002; **294**: 949–955.

24. Kapust RB, Tozser J, Fox JD, Anderson DE, Cherry S, Copeland TD, Waugh DS. Tobacco etch virus protease: mechanism of autolysis and rational design of stable mutants with wild-type catalytic proficiency. *Protein Eng.* 2001; **14**: 993–1000.

25. Mohanty AK, Simmons CR, Wiener MC. Inhibition of tobacco etch virus protease activity by detergents. *Protein Expr. Purif.* 2003; **27**: 109–114.

26. Wüthrich K. *NMR of Proteins and Nucleic Acids*. Wiley-Interscience: New York, 1986.

27. Wishart DS, Sykes BD, Richards FM. Relationship between nuclear magnetic resonance chemical shift and protein secondary structure. *J. Mol. Biol.* 1991; **222**: 311–333.

28. Palmer AG. NMR Probes of molecular dynamics: Overview and comparison with other techniques. *Annu. Rev. Biophys. Biomol. Struct.* 2001; **30**: 129–155.

29. Brown LR, Bösch C, Wüthrich K. Location and orientation relative to the micelle surface for glucagon in mixed micelles with dodecylphosphocholine: EPR and NMR studies. *Biochim. Biophys. Acta* 1981; **642**: 296–312.

30. Wüthrich K, Billeter M, Braun W. Polypeptide secondary structure determination by nuclear magnetic resonance observation of short proton-proton distances. *J. Mol. Biol.* 1984; **180**: 715–740.

31. Zerbe O, Neumoin A, Mares J, Walser R, Zou C. Recognition of neurohormones of the NPY family by their receptors. *J. Recept. Sig. Transd.* 2006; **26**: 487–504.

32. Bader R, Bettio A, Beck-Sickinger AG, Zerbe O. Structure and dynamics of Micelle-bound Neuropeptide Y: Comparison with unligated NPY and implications for receptor selection. *J. Mol. Biol.* 2001; **305**: 307–329.

33. Bettio A, Dinger MC, Beck-Sickinger AG. The neuropeptide Y monomer in solution is not folded in the pancreatic- polypeptide fold. *Protein Sci.* 2002; **11**: 1834–1844.

34. Cowley DJ, Hoflack JM, Pelton JT, Saudek V. Structure of neuropeptide Y dimer in solution. *Eur. J. Biochem.* 1992; **205**: 1099–1106.

35. Sargent DF, Schwyzer R. Membrane lipid phase as catalyst for peptide-receptor interactions. *Proc. Natl. Acad. Sci. U.S.A.* 1986; **83**: 5774–5778.

36. Schwyzer R. Membrane-assisted molecular mechanism of neurokinin receptor subtype selection. *EMBO J.* 1987; **6**: 2255–2259.

37. Moroder L, Romano R, Guba W, Mierke DF, Kessler H, Delporte C, Winand J, Christophe J. New evidence for a membrane-bound pathway in hormone receptor binding. *Biochemistry* 1993; **32**: 13551–13559.

38. Wimley WC, White SH. Experimentally determined hydrophobicity scale for proteins at membrane interfaces. *Nat. Struct. Biol.* 1996; **3**: 842–848.

39. Ridder AN, Morein S, Stam JG, Kuhn A, de Kruijff B, Killian JA. Analysis of the role of interfacial tryptophan residues in controlling the topology of membrane proteins. *Biochemistry* 2000; **39**: 6521–6528.

40. Park JH, Scheerer P, Hofmann KP, Choe HW, Ernst OP. Crystal structure of the ligand-free G-protein-coupled receptor opsin. *Nature* 2008; **454**: 183–187.

41. Warne T, Serrano-Vega MJ, Baker JG, Moukhametzianov R, Edwards PC, Henderson R, Leslie AG, Tate CG, Schertler GF. Structure of a beta1-adrenergic G-protein-coupled receptor. *Nature* 2008; **454**: 486–491.

42. Lindner D, Walther C, Tennemann A, Beck-Sickinger AG. Functional role of the extracellular N-terminal domain of neuropeptide Y subfamily receptors in membrane integration and agonist-stimulated internalization. *Cell. Signalling* 2008 (in press).